INSTITUT DE FRANCE
Académie des sciences

Comptes Rendus
Physique

Anthony Boccaletti

Observations of circumstellar disks in scattered light with SPHERE at the VLT

Published online: 21 March 2023

https://doi.org/10.5802/crphys.134

Part of Special Issue: Exoplanets
Guest editors: Anne-Marie Lagrange (LESIA, Observatoire de Paris, Université PSL, CNRS, Sorbonne Université, Sorbonne Paris Cité, 5 place Jules Janssen, 92195 Meudon, France.) and Daniel Rouan (LESIA, Observatoire de Paris, Université PSL, CNRS, Sorbonne Université, Sorbonne Paris Cité, 5 place Jules Janssen, 92195 Meudon, France.)

Les Comptes Rendus. Physique *sont membres du*
Centre Mersenne pour l'édition scientifique ouverte
www.centre-mersenne.org
e-ISSN : 1878-1535

Comptes Rendus
Physique
Published online: 21 March 2023
https://doi.org/10.5802/crphys.134

Exoplanets / *Exoplanètes*

Observations of circumstellar disks in scattered light with SPHERE at the VLT

Observations des disques circumstellaires en lumière diffusée avec SPHERE au VLT

Anthony Boccaletti[a]

[a] LESIA, Observatoire de Paris, Université PSL, CNRS, Sorbonne Université, Sorbonne Paris Cité, 5 place Jules Janssen, 92195 Meudon, France

E-mail: anthony.boccaletti@obspm.fr (A. Boccalettit)

Abstract. The technological developments initiated in the early 21st century have led to the implementation of "planet finders" instruments on 8-m class telescopes which are in operation since 2014-2015. Such facilities are at the inception of significant progresses in the study of exoplanetary systems by enabling high contrast imaging of the environment of young nearby stars. One of the most productive science in this field is certainly the observations at high angular resolution of circumstellar disks, from the very young gas-rich protoplanetary disks all the way to more elusive dust-rich debris disks. In this paper, we summarize the main results obtained for these two categories of objects focusing on their morphological characteristics, as well as on the measurement of optical properties of the small dust particles to which the near IR spectral range is sensitive to. We mostly provide exemples based on observations performed with the SPHERE instrument at the VLT.

Résumé. Les développements technologiques initiés au début du 21ème siècle ont conduit à la mise en place d'instruments "découvreurs de planètes" sur des télescopes de la classe 8m en fonctionnement depuis 2014-2015. De telles installations sont à l'origine de progrès significatifs dans l'étude des systèmes exoplanétaires en permettant l'imagerie à haut contraste de l'environnement des jeunes étoiles proches. L'une des sciences les plus productives dans ce domaine est certainement l'observation à haute résolution angulaire des disques circumstellaires, depuis les très jeunes disques protoplanétaires riches en gaz jusqu'aux disques de débris plus insaisissables, riches en poussières. Dans cet article, nous résumons les principaux résultats obtenus pour ces deux catégories d'objets en nous concentrant sur leurs caractéristiques morphologiques, ainsi que sur la mesure des propriétés optiques des petites particules de poussière auxquelles la gamme spectrale du proche IR est sensible. Nous présentons surtout des exemples basés sur des observations réalisées avec l'instrument SPHERE au VLT.

Keywords. Circumstellar disks, planet formation, exoplanets, high contrast imaging, polarimetric imaging.

Mots-clés. Disques circumstellaires, formation des planètes, exoplanètes, imagerie haut contraste, imagerie polarimétrique.

Note. Follows up on a conference-debate of the French Academy of Sciences entitled "Exoplanets: the new challenges" held on 18 May 2021, visible via
https://www.academie-sciences.fr/fr/Colloques-conferences-et-debats/exoplanetes.html.

Note. Fait suite à une conférence-débat de l'Académie des sciences intitulée « Exoplanètes : les nouveaux défis » tenue le 18 mai 2021, visible via
https://www.academie-sciences.fr/fr/Colloques-conferences-et-debats/exoplanetes.html.
Published online: 21 March 2023

1. Introduction

Understanding how and when planets form is a central question in the study of exoplanets. In the current paradigm, mostly based on Solar System observations, a stellar system emerges from the gravitational collapse of a gaseous cloud, which leaves a protostar in the center and a disk of gas and dust orbiting the star in a nearly flat distribution, owing to the conservation of angular momentum. Dust will grow from sub micron-size to form pebbles [1], which after a series of accretion and collision interplays can produce km-size bodies, i.e. the planetesimals [2, 3]. Oligarchic growth [4] can explain how these planetesimals will end up in massive planetary cores (likely a few $M_\oplus$), and finally, these cores will accrete gas [5] resulting in the formation of giant planets. This whole process of "core accretion" is estimated to last about 1 Myr or so, after which the gas is dissipated by photo-evaporation [6], or integrated into the atmospheres of giant planets. This scenario (see details in [7]) provides the big picture, but one lesson from exoplanets searches is clearly the diversity of their properties. For instance, some alternative models to the core accretion scenario have been proposed, like the gravitational instability [8], which is able to generate giant planets more rapidly and directly from the collapse of the gas in the protoplanetary disk, in a sort of small-scale stellar formation mechanism. It is not unlikely that several mechanisms take place among stellar systems or even in a same system.

Two means can be considered to address the context of planet formation from the observation of the exoplanet population. First, we can study statistically the orbital properties (semi major axis, inclination, eccentricity), and the bulk properties (mass, radius, hence density) of known planets, and compare it to synthetic planet population models [9]. Another way consists in measuring their composition to derive chemical constraints on the abundance of elements in comparison with planet formation models [10]. These two aspects require to characterize beforehand the environment in which planets form and evolve to provide inputs to these planet formation models.

In the early stage, a system contains large amount of gas and dust (with a typical 100:1 ratio) in the form of a protoplanetary disk, also known as a "planet forming disk", which can determine locally the composition of a planet, or even its fate given that planets interact with the gas, and migrate inward or outward [11]. Mature systems, which represent the vast majority of known exoplanets, have experienced significant dynamical evolution, so that the determination of the conditions of their formation is not straightforward. For this reason, observing the systems when they are just a few million year old is more relevant to put constraints on planetary formation. Protoplanetary disks have complex morphologies as a result of gas dynamics and size-dependent coupling with dust particles, eventually leading to planet formation. In a later stage, when the system evolves and the gas dissipates, planetesimals become the most abundant objects. Collisional cascades among the planetesimals produce second generation micron-sized grains, hence the term of "debris disk" [12]. Like in the Solar System the planetesimals are distributed in the form of belts, similar to the Kuiper and the asteroid belts, and located at a few tens of astronomical units (AU) from the star.

Historically, the first disks were identified from the excess emission that the dust produces at infrared wavelengths, like the so-called Vega phenomenon [13–15], the emission peak being proportional to the temperature of the grains, and thus to the stellocentric distance of the

dust, together with its optical properties. The IRAS satellite has been instrumental in detecting such signatures (in excess compared to the blackbody-like emission of a single star, see Fig. 1) at IR wavelengths of 10 to 100 μm typically, and interpreted as either protoplanetary disks (near/mid IR emission, high fractional IR luminosity) or debris disks (far IR emission, low fractional IR luminosity). However, the spectral energy distribution (SED) of a system derived from photometric measurements carries important degeneracies related to its geometry (single belt, multiple belts, continuous disk with or without cavity) and to the dust properties (emission depends on temperature, size, shape, and composition of grains) [12].

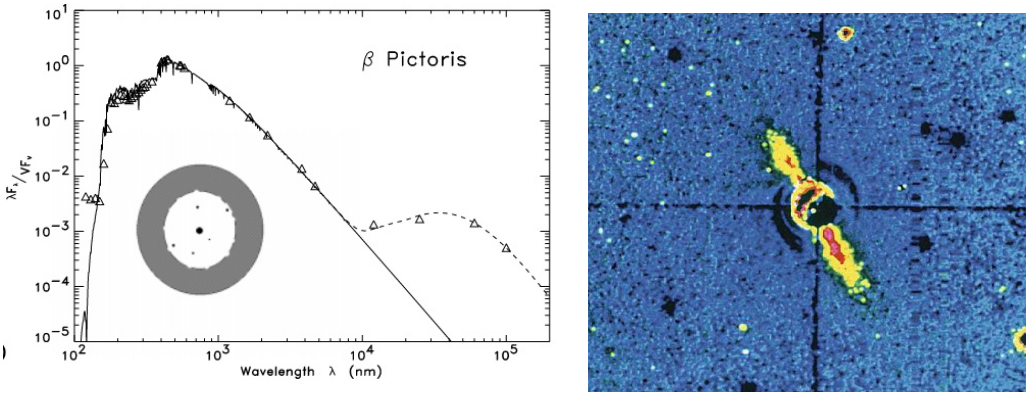

Figure 1. Spectral Energy Distribution of β Pictoris measured with IRAS (left), and first image of the debris disk observed with a 2.5-m telescope at 850 nm and with a 7″ diameter coronagraph [16] (right). The FoV is about 92″x82″.

Given the aforementioned characteristics, and because exoplanetary systems have AU-scale dimensions, imaging disks with high angular resolution and high sensitivity has been decisive to characterize them further, both in scattered light at visible and near IR wavelengths, as well as in thermal emission at millimetric wavelengths. The first image of a debris disk was obtained in the early 80s from the ground, around the famous star β Pic, featuring a favorable combination of proximity, size, luminosity and inclination [16]. It took more than a decade to achieve similar level of performance on other systems, thanks to the HST [17–20], while on the ground the sensitivity has been a strong limitation [21] until the implementation of adaptive optics on 8-m class telescopes. Taking advantage of an angular resolution of 40-50 mas corresponding to a few AU for the nearest stars like β Pic, to a few tens of AU in the main young star associations at 100-150 pc, the exploration of the brightest disks unveiled a rich morphology with spirals, gaps, and rings [22–30]. Unsurprisingly, this breakthrough in disk imaging coincides with the first obtained images of extrasolar giant planets [31–36] (see [37] this proceeding for a review of exoplanet imaging results and projects).

A revolution came with extreme adaptive optics facilities (so called “planet finders”) combined to optimized coronagraphs, and also because significant efforts were invested in the observational and data reduction strategies [38]. The instruments SPHERE at the VLT [39], GPI at Gemini [40], and SCExAO at Subaru [41] were prolific to resolve structures in protoplanetary and debris disks in scattered light, shedding light on how the matter is distributed in the first stages of planetary formation. The morphology and the fine structures distribution of millimeter dust and

gas in protoplanetary disks is also revealed owing to radio-interferometry with ALMA which provides complementary informations about those exosystems with a similar angular resolution as SPHERE [42, 43].

This paper focuses exclusively on the measured properties of circumstellar disks recently observed in scattered light, based in particular on examples from SPHERE observing programs, although not exhaustively.

2. Detection methods

Circumstellar disks are intrinsically angularly small, and faint, featuring a large contrast (>10^{-3}, defined as the ratio between the intensity of an object in the field and the host star) with respect to the central star, hence require large telescope diameters, high sensitivity and high dynamic to be observed. Therefore, the techniques for disk imaging and exoplanet imaging are identical, both being off-axis, resolved or unresolved, objects with respect to the optical axis defined by the star (assumed unresolved). In that respect, an extreme adaptive optics (AO) system like SPHERE is able to routinely achieve Strehl ratio larger than 80% in the near IR (J, H and Ks bands) for bright stars (R<10) and can even provide a Strehl of 50% at visible wavelengths for R<9 [44], allowing to deliver exquisite image quality with angular resolution of 15 to 50 mas for wavelengths in the range 0.6-2.0 μm. Such a low wavefront error level is necessary for a coronagraph to provide a large rejection of the starlight (see [45] this proceeding for a review of coronagraphic techniques). The SPHERE coronagraph [46] has a diameter of about 0.2″ which means that no off-axis object can be recovered below the Inner Working Angle of ~ 0.1″. Raw contrasts measured with SPHERE are typically reaching $10^{-3} - 10^{-4}$ in separation range $0.1 - 0.3''$, and better than 10^{-4} between 0.3″ and the correction radius at ~ 0.8″ (see [39, Fig. 10]).

To reach a contrast that is compatible with exoplanet or disk imaging, the residual starlight left behind the coronagraph must be further removed or at least attenuated. This starlight pattern is a complex mixture of diffraction effects which can be static, highly variable, or quasi-static, the latter being the more difficult to get rid of. In conjunction with the improvement of AO systems, several techniques, combining observing strategies and numerical methods, were developed with the purpose to calibrate the stellar light, independently of the off-axis object to detect. For disk imaging, this can be accomplished in three different ways, taking advantage of data diversity introduced by a specific observing mode in order to disentangle the starlight from astrophysical sources around the star, and taking into account the properties of these sources.

The most obvious technique relies on the observation of one or several reference stars observed in the same configuration as the science target, usually in a short time frame to ensure a somehow similar starlight pattern. The so-called reference star differential imaging (RDI) has been very successful with the HST (Fig. 2), in an atmosphere-free environment where the global wavefront is highly stable. In fact, following the discovery of the β Pictoris debris disks, the first scattered light disk images at high angular resolution, were obtained with RDI [17, 18]. The method was generalized later to using a set of reference stars, with for instance linear combinations of frames and Principal Component Analysis, which allowed to discover a few more disks left undetected in archival HST data [47, 48]. On the ground, because of the atmospheric turbulence, but also due to the inevitable gravity related variations of the optical wavefront, RDI has been much less effective until recently [49]. However, advanced numerical techniques, like artificial intelligence, are now being deployed to tackle this challenge since the amount of data, hence potentially of reference frames, is just gigantic.

A second technique, devised for exoplanet detection, is taking advantage of the field rotation at the focus arising from the alt-azimuthal mount configuration in large telescopes or rolls with space telescopes (Fig. 2). If the wavefront errors are mostly coming from a pupil plane the net

effect is that an off-axis object rotates in the image as the parallactic angle, while most of the starlight is fixed, or evolves differently (with the exception of the aberrations caused by high altitude winds). As such, Angular Differential Imaging ([50, ADI]) has been used for detecting all the directly-imaged exoplanets known today and comes with various flavors of data processing techniques [51, 52]. An important aspect of ADI is that it implies a self-subtraction of the object to detect, as long as this object contributes, even in a small fraction, to the construction of the reference frame(s) to be subtracted to the data set. For a planet, which can be modeled as a point source, the self-subtraction can be taken into account to measure its photometry, but the problem is far more complex for an extended structure like a disk. In that case, the self-subtraction depends on the morphology of the object which is basically what we are trying to measure [53]. As a result, we have to assume a particular morphology and perform forward modeling to recover the disk geometric parameters and then its optical properties [54]. While this is doable for debris disks which can be approximated as a belt (or multiple belts) and providing the inclination is relatively large, it is totally unpractical for protoplanetary disks. In practice, we are only measuring departures to an azimuthally-symmetrical geometry. To get around this problem some algorithms have been recently proposed to attempt preserving at most the flux of an extended object [55, 56]. Still, performing direct measurements of complex structures around stars with ADI remains challenging and could lead to wrong interpretations of the morphology: streamers can be seen at the edge of a highly inclined debris disk belt as an amplification in one direction of the disk halo [57], or rings and spirals can be pinched in some directions as a result of the disk minor axis rotating slower than the outer part combined to the effect of the scattering phase function [58]. Both ADI and RDI can be used with either IRDIS the camera of SPHERE and IFS the low resolution spectro-imager, providing spectral information from 0.95 to 2.3 μm.

Finally, the third technique benefits from the polarization of the light induced by the scattering of the starlight by dust grains, while the starlight itself is generally unpolarized. Therefore, filtering the linearly polarized signal in the image of an exosystem is highly efficient to reduce the contribution from the star and to reveal the dust contribution. Dual Polarization Imaging (DPI, also referred as Polarimetric Differential Imaging) is implemented in SPHERE IRDIS but is only available in broad band or narrow band filters. Unlike ADI, the morphology of the disk is fully preserved, but as a drawback the beam splitter and the polarizers implemented in SPHERE transmits only 50% of the light, while the polarized signal of a disk is also intrinsically smaller (usually a few tens of % of the unpolarized flux). DPI comes also with a series of observational constraints but combining DPI and pupil tracking can circumvent these issues, and provides simultaneously for the same data set the polarized and unpolarized image [59, 60]. Yet, DPI imaging has been extremely efficient for resolving structures in the vast majority of protoplanetary disks observed with SPHERE [61].

3. Characterization of protoplanetary disks

Protoplanetary disk is a generic term which corresponds to the phase between the formation of the star and the transition to the debris disk phase when the gas is dissipated. This period probably lasts a few Myr during which the system can undergo significant evolution which impacts the disk structuring. Unresolved photometry in the near to far IR has provided in the past some hints about the structures in these disks, in particular the presence of cavity or gaps, which shows up as features in the SED of these systems owing to the temperature-distance dependence. Imaging is able to retrieve much more details in the morphology, and allows to leave some degeneracies when modeling the SED. All disks observed in scattered light have structures. If they don't, it is essentially because they are too small and/or too faint given the sensitivity [58]. Structures are easier to detect in polarimetry if the disk is nearly face-on, while at

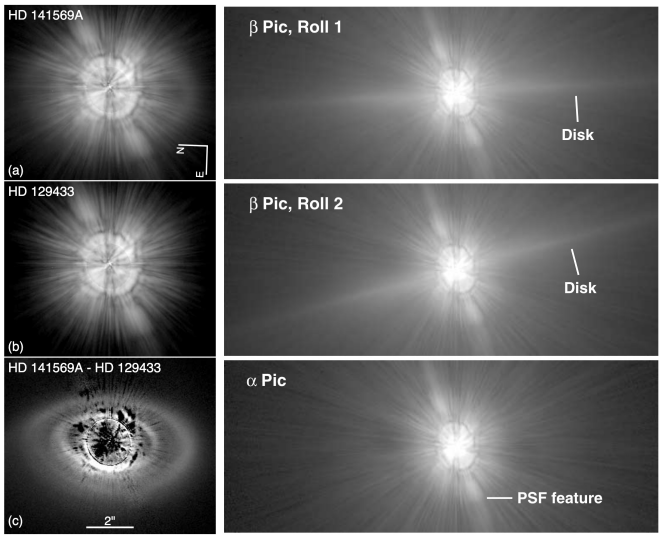

Figure 2. Illustrations of the RDI (left) and ADI (right) methods from the same instrument: ACS on HST. The ACS PSF being strongly aberrated, the coronagraphic images that are displayed here are very extended. The left panel shows an observation of HD 141569 and a reference star together with the subtraction revealing the gas-rich debris disk [22]. The right panel is an observation of the disk of β Pic observed at two roll angles, demonstrating the stability of the coronagraphic diffraction pattern with respect to the disk itself which rotates with the field [62].

high inclinations the effect due to the phase function or the spatial distribution of the dust can be degenerated. In the case of protoplanetary disks, combining observations in the near IR and millimeter wavelengths is crucial to test formation theories because the two regimes are sensitive to different sizes of dust particles (sub-micron, and millimeter respectively), the distribution of which can differ during the evolution of a system. For instance, small particles are efficiently coupled to the gas while the largest are not. Therefore, we can observe different distributions and dynamics with SPHERE and ALMA. Below, we discuss the main structures that we manage to observe in scattered light.

3.1. *Spirals*

Spirals can be the result of density waves being launched by a planet orbiting the star and propagating in the gas [63]. Near IR observations in scattered light are sensitive to micron-size grains which are strongly coupled to the gas, so these images are effectively tracing the perturbation in the gas distribution. One of the first protoplanetary disk observed with SPHERE, MWC 758 [64], has two prominent and almost symmetrical spirals which totally dominate the scattered light image. These patterns can be interpreted using the linear theory of wave density [65] as being induced by a gravitational perturber in Keplerian rotation around the star, so presumably a planet. The linear relation to describe the shape of a spiral in polar coordinates $\theta(r)$ (r being the radial distance to the star), as a function of the planet location (r_c, θ_0) and disk properties reads as follows [66]:

$$\theta(r) = \theta_0 - \frac{\mathrm{sgn}(r-r_c)}{h_c} \times \left[\left(\frac{r}{r_c}\right)^{1+\beta} \left\{ \frac{1}{1+\beta} - \frac{1}{1-\alpha+\beta} \left(\frac{r}{r_c}\right)^{-\alpha} \right\} - \left(\frac{1}{1+\beta} - \frac{1}{1-\alpha+\beta} \right) \right] \quad (1)$$

The linear theory is convenient in the context of direct imaging as it provides an analytical expression of the spiral shape being a function on the planet location, the angular velocity and the disk aspect ratio (scale height divided by the radius), hence related to the gas temperature. The properties of the disk are contained in the parameter α and β, which are the exponents of the power law describing the variation of the angular velocity $\Omega \propto r^{-\alpha}$, and the sound speed $c_s \propto r^{-\beta}$. The fit of this relationship in MWC 758 (Fig. 3), but also HD 135344B [67] images, leads to several solutions with either inner or outer planets. The case with inner planets yields large aspect ratios corresponding to unphysical temperatures, so that the scenario with outer planets is usually favored. The same conclusion is reached based on hydrodynamical models in which a pair of a so-called "grand-design" spirals can be generated by a single perturber [63]. In complement, direct imaging in unpolarized light with SPHERE allows to put strong constraints on the presence of giant planets (undetected in polarized light) in these systems with more sensitivity at large separations, precisely where the presence of planets is favored by the analysis of spiral arms. However, no planet was discovered yet in these systems. For instance, the SPHERE data achieve detection limits as low as 1~2 M_J for HD 135344B [68] and MWC 758 [69].

As of today we never identified a bona-fide planet related to a spiral arm, with the exception of HD 100453 [70, 71], in which the perturber is not a planet but a low-mass star. In the context of findings connection between spirals and planets, the even more complex system AB Aur is unique to understand this connection, because it is one out of the two cases where a pair of spirals is detected both in scattered light and in CO gas with ALMA [72]. Two independent observations reported hints of the presence of two protoplanets possibly associated to the spiral arms. First, with SPHERE in polarimetry, the eastern spiral features a twist which matches relatively well the classical spiral model, this twist being the place where the inward and the outward spiral components are launched [73] (Fig. 4). Second, based on SCExAO data, a diffuse region at the tip of the western spiral has been modeled as a combination of a protoplanet emission and scattering from the disk [74], the location of which is also in line with ALMA observations [72]. The disk around HD 169142 was also scrutinized with SPHERE with very aggressive processing to remove the starlight which allowed to detect or re-detect several blobs inside the complex spiral pattern of this disk. Since these disk features also move at Keplerian velocity [75] the connection to planets is still to be demonstrated.

Dynamically, being waves, spirals are expected to rotate at the same angular velocity as the source, and as such can appear to move at a super-Keplerian speed outwards of the launching site, or sub-Keplerian inwards. However, it is challenging to obtain a precise measurement, especially for outer planets simply because the orbital period can be as large as a few hundred years, while an inner planet may produce a visible motion in a few years. We note that in the case of MWC 758 the extreme reproducibility of SPHERE images and the knowledge on the field orientation allowed to derive a rotation of 0.22° consistent with an outer perturber at 172 AU [76] still to be discovered. Follow up of other systems, in particular AB Aur may allow to better constrain the origin of spirals.

Most of the disk with spirals were observed face-on because it is the most efficient case in DPI with SPHERE, but in a few cases, based on a comparison to radiative transfer models, we were able to identify spirals in more inclined disks, like for RY Lup [77]. Interestingly, for RY Lup and also T Cha [78], the direction of polarization is not fully azimuthal, indicating that multiple scattering occurs within the dusty disk.

Overall, the connection between spirals and planets is not fully confirmed. Spirals can also arise from gravitational instabilities which can develop when the disk is self-gravitating [79], under the conditions that the disk is more massive than a quarter of the star's mass. The aforementioned systems are not expected to be that massive. However, some disks like AB Aur (Fig. 4) and HD 100546 show a variety of spirals morphologies which may have a different origin,

possibly self-gravity [58, 73].

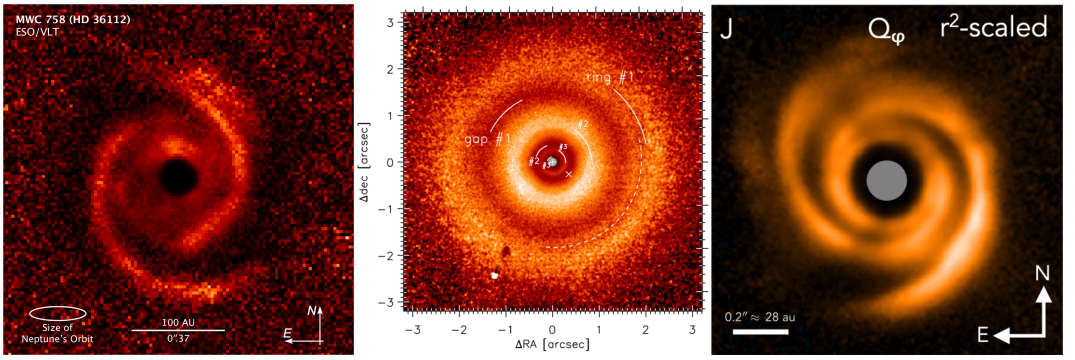

Figure 3. Images obtained with SPHERE illustrating main features observed in protoplanetary disks in scattered light (from left to right): the spiral arm of MWC 758 [64], the rings/gaps in TW Hya [80], and the shadows in HD 135344 B [67].

3.2. *Rings and cavities*

Cavities and rings in systems featuring IR excess were very soon suspected from the dip in the excess at near IR wavelengths. The dust depletion at short stellocentric distances can be the result of photo-evaporation, dust evolution, or gravitational sweeping by massive bodies like planets, the latter being frequently involved as an argument to target such systems in high-contrast imaging surveys [81]. Cavities are found in most protoplanetary and transition disks observed in scattered light with SPHERE. Like spirals, the rings and cavities are easier to detect at moderate disk inclinations with either DPI and/or ADI, as showcase with the images in both polarized and unpolarized intensity of HD 97048 [82] and RXJ 1615 [83]. Their size can be different than in the millimeter regime indicative of dust segregation which may be explained by dust trapping by planets at the gap edges. With sizes in the range $\sim 200-400$ AU, and inclinations of $40-50°$, the fitting of ellipses to the multiple rings detected in these systems allows to directly measure the scale height which can be as large as 15 to 20 AU (measured at 100 AU). Such large values are related to the fact that scattered light is sensitive to the surface of the disk (corresponding to optical depth $\tau = 1$). In nearly face-on geometries, alternation of rings and gaps was also evidenced owing to differential polarimetry in the disk around TW Hya [80] or HD 169142. [84]. In that cases, surface density can be inferred from surface brightness radial variations. The gaps in TW Hya (Fig. 3) are found to be relatively shallow which would imply a few to tens Earth-masses perturbers if they have a gravitational origin. Since such planets are not yet detected, other scenarios involving the accumulation of dust particles at snowlines are still plausible [85].

There are a few examples for which a cavity can be directly connected to one or more perturbers, most are low mass stars like for HD 142527 [86] and GG Tau [87] (Fig. 4). In the latter, the remarkable precision delivered by SPHERE allowed to interpret the many fine structures at the edges of the cavity with hydrodynamical models as being triggered by periodic perturbations of the central binary star. The case of PDS 70 [88–91] is certainly the most relevant in this category since at least two giant planets have been identified in the cavity orbiting respectively at 22 AU and 35 AU while the cavity is 55 AU wide. These very young objects still in a formation phase [92] are presumably sculpting the disk.

3.3. *Shadows*

Direct imaging and in particular DPI has also revealed shadow patterns in some of the brightest protoplanetary disks. Shadows are systematically associated to large near IR excess which is in line with the fact that they take origins in the inner part of these systems due to inner belts casting shadows in the outer parts. One of the first example was found in the disk of HD 142527 which features a very large cavity and two localized centro-symmetrical shadows in the outer belt at the northern and the southern tips. They are observed both in the visible [93] and near IR [94] and explained using radiative transfer with an optically thick disk close to the star and warped by 70° with respect to the outer one [95]. Similar conclusions were reached for the shadows of HD 100453 [96] with the particularity that these shadows are apparently connected to two spirals. Although these spirals are likely gravitationally triggered by an outer M star companion, the shadows may also play a particular role here. Finally, shadows can have much more complex structures than just two anti-symmetrical dark regions casted on an outer belt, as in SAO 206906 where several shadows feature azimuthal variations at different epochs (Fig. 3), reminiscent of material in rotation at much closer orbital radius [67].

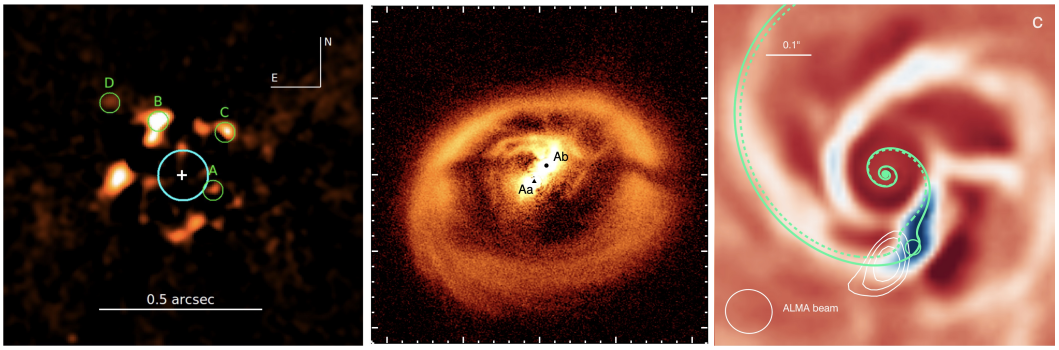

Figure 4. Typical small-scale structures: blobs in HD 169142 [75], cavity and multiple spirals in GG Tau [87], spiral twist in AB Aur [73].

4. Characterization of debris disks

The debris disk phase is referring to the next stage in the evolution (the typical age is 10~15 Myr) of planetary systems when most of the gas is dissipated and large bodies are formed. The system becomes dominated by gravity so that collisions among planetesimals produce “second-generation” dust particles down to micron sizes. As a result, the dust is mostly generated in one or several belts where the planetesimals collide. Because debris disks are intrinsically faint, polarimetric imaging is less efficient than for protoplanetary disks but remains the only option for disks seen at low inclination. On the contrary, non polarimetric imaging is also used more frequently as long as the disk morphology is easier to describe with parametric models and the use of forward modelling. This observing mode strongly bias the detection towards highly inclined disks. High contrast imaging can essentially constrain their morphology (possibly with temporal resolution) and the optical properties of dust particles. Hereafter, we summarize the main physical characteristics of debris disks that are derived from observations.

4.1. *Morphology and interaction with planets*

For most known cases, debris disks are dust belts typically located at a few tens of AU from the star. The disk around HR 4796 as observed with SPHERE [97] gives a clear example of such an evolved system. It is relatively straightforward to estimate its size, its inclination (the angle with respect to a face-on orientation) and its position angle (rotation in the plane of the sky with respect to the North). As such, direct imaging of debris disks provides unambiguous measurements of the locations of planetesimals, which once compared to previous estimations made from SEDs, lead to large discrepancies, as a clear proof that the latter is subject to degeneracies between temperature and dust location. Belts in debris disks are usually rather sharp, especially at their inner boundary which calls for the presence of a perturber shepherding the edge of the disk due to its chaotic zone [98], although several planets would probably be needed to explain the large cavity observed in debris disks. No such connection between a planet and the sharp edge of a disk has been evidenced so far. On the contrary, the outer intensity slope of debris disk belts usually goes like r^{-4} (r being the physical separation to the star), which is the characteristics of dust particles blown away by the radiation pressure. A sharper slope may indicate truncation by an object outwards of the belt like for HR 4796 [97].

Generally speaking, it is tantalizing to seek for any departure to this simple belt geometry since any non centro-symmetrical features could be the result of gravitational perturbations by planets, and could thus be used as an indirect signature of their presence. Indeed, the spatial structure and then the scattered light image of a debris disk can be strongly affected by the presence of planets as illustrated in some theoretical works [99], depending on the disk inclination and planet's eccentricity. A case study is the system β Pic, an edge-on debris disk, in which a warp has been identified in the first AO+coronagraph images [100], and interpreted as the presence of a $\sim 10\,M_J$ giant planet at ~ 10 AU on an inclined orbit (4-5°). The planet was confirmed a decade later [33], the properties of which are matching very well the predictions. While mostly all directly imaged planets are found in young systems, which also contain a dust component, only one other example, (with the exception of the much younger PDS 70 system), features a planet and a debris disk in the same image: HD 106906 [101]. However, this planet is found at a larger angular separation from the star (corresponding to 650 AU in projection), but the fact that the disk belt is resolved allows to infer a much larger physical distance of 2000-3000 AU [102] (if the planet and the disk were coplanar) suggesting an ejection mechanism.

An interesting outcome of SPHERE observations is the case of debris disks around HIP 73145 [103], NZ Lup [104], and HIP 67497 [105] which features at least two or multiple belts, together with the more complex HD 141569 in which many rings, ringlets and broken structures have been detected [106]. One plausible explanation is that such multiple-ring geometries are generated by instabilities rather than shaped by planets, for instance based on the so-called "photo electric" effect [107], which implies that the gas compound is not negligible in these system with gas to dust ratio close to unity. CO gas was detected at least in HIP 73145 and HD 141569, with the latter being categorized as a gas-rich debris disk and showing a very strong match between the gas and dust distribution [108, 109]. To explain this it has been shown that collisions within planetesimals in a belt can release both second generation dust and gas explaining their colocation [110].

On the other hand we expect massive collisions between very large asteroids or small planets to occur in a young planetary system, leaving a reservoir of dust at the place of the release, which would be detected in scattered light images as brightness asymmetries [111]. Such a mechanism has been posited to explain asymmetric features in several debris disks although without firm conclusions [109, 112].

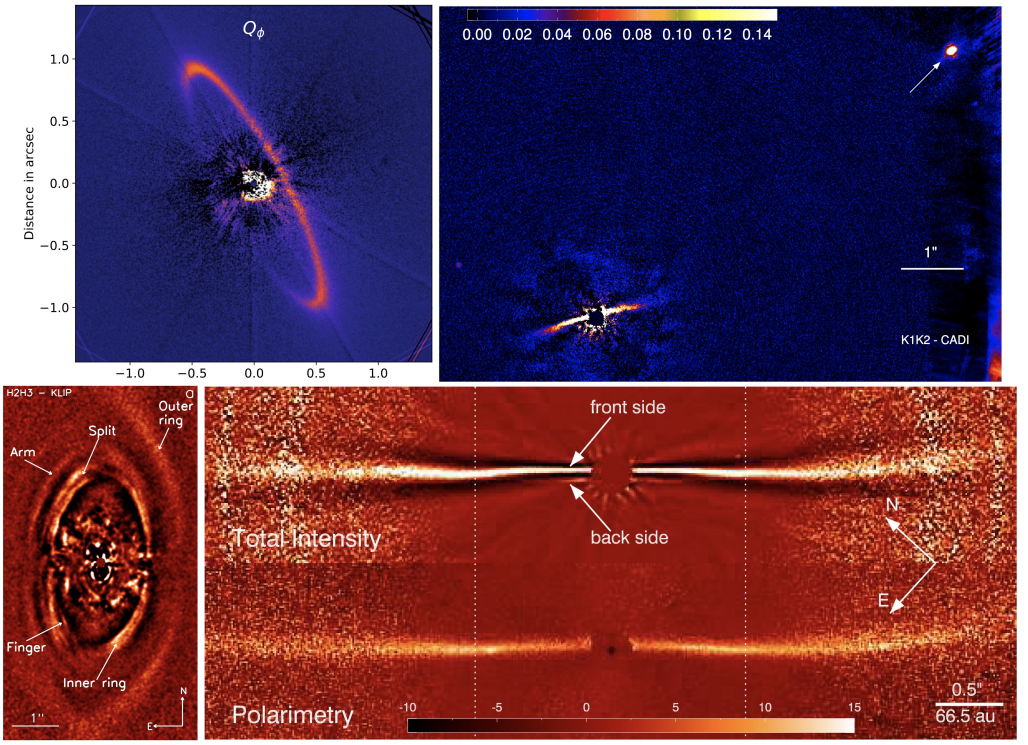

Figure 5. Exemple of debris images illustrating some of their morphological characteristics (from left to right, top to bottom): the planetesimals belt of HR 4796 observed in visible polarimetry [113], the ring and the planet of HD 106906 [102], the multiple rings and ringlets in the gas-rich debris disk of HD 141569 [106], and the highly inclined disk of HD 32297 [54] in total intensity and in polarimetry showing halo beyond the birth ring (dashed line).

4.2. *Scattering phase function*

In the generic case of a debris disk with a single belt seen at a given inclination, the intensity (relative to the star) along the belt varies with the scattering angle. This scattering phase function can be measured to derive optical properties of the dust grains as long as we assume the disk to be infinitely thin, with an azimuthally constant surface density, although we can expect departure from this simple hypothesis [112]. Both non polarimetric and polarimetric data are useful in this case in providing complementary informations, with the problematic that non polarimetric data are affected by self-subtraction modifying the disk intensity, so special care is needed in that case, for instance using forward modeling as long as the disk geometry can be described by a few parameters, or ideally, RDI processing. Because it is bright and seen at a favorable inclination, the disk around HR 4796 has been extensively studied in this context [97, 113]. The scattering phase function can be measured at small scattering angles (down to 13.6°) which is decisive to test various dust properties (Fig. 7). On the contrary, the polarized scattering phase function is rather flat at small scattering angles. The phase functions measured for HR 4796 and other disks like GSC 07396-00759 [114], HD 32297 [54] and HD 15115 [115] show that Mie scattering of compact grains are not compatible with the observations, favoring particle aggregates as opposed to compact spheres. In the case of HR 4796, to account for the amount of back scattering, the modeling

of the scattering phase function suggests that grains are bigger than the observing wavelength. In a general case, it is found difficult to reproduce the scattering phase function with the standard Henyey–Greenstein function but it often requires multiple components. Equations 2 and 3 provide the analytical expression of these functions in total intensity and polarized intensity respectively, where g is the aninostropic scattering factor, and θ is the scattering angle.

$$f_{Itot}(\theta) = \frac{1-g^2}{4\pi(1+g^2+2g\times\cos(\theta))^{3/2}} \tag{2}$$

$$f_{Ipol}(\theta) = f_{Itot}(\theta) \times \frac{1-\cos(\theta)}{1+\cos(\theta)} \tag{3}$$

For illustration, a model of a disk image in scattered light, the SPF of which is defined by Eq. 2, is shown in Fig. 6, for several inclinations and anisotropic scattering factors.

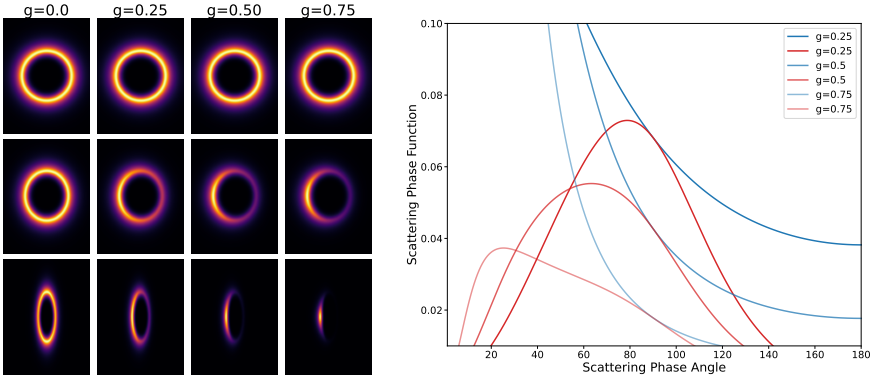

Figure 6. Left: disk models in total intensity for several g values and inclinations (i=0°, 30°, 70° from top to bottom). Right: scattering phase functions and polarized scattering phase functions for several g values.

Dust production is also a feature of comets in the Solar System which can be studied from a different perspective, sometimes in-situ, so there has been some attempts to compare the properties of dust in these two kind of objects to identify common optical properties hence to put constraints on the dust particles in debris disks in terms of size, shape and composition [116].

4.3. *Spectroscopy*

SPHERE and other planet finders provide spectro-imaging capabilities at low resolution in the near IR extensively used for exoplanet characterization. In the case of disks, the spectral information has been mostly useful to process the data and reveal substructures [75] since retrieving the spectral information in non polarimetric data involves a careful modeling to circumvent the problematic of self-subtraction, and necessarily suffer from a lower signal to noise ratio than in imaging. This has been doable in a very few cases like the bright disk of HD 32297 [54] for which the negative slope (blue color) of the spectrum is compatible with sub-micron dust particles (Fig. 7). This in line with the global picture of debris disks around A type stars in which small dust grains are put on very eccentric orbits or even blown out by the radiation pressure. Given the very high inclination of this disk, the spectrum is likely dominated by these grains that are seen along the line of sight everywhere in the disk image. On the contrary, HR 4796 has a red spectrum indicative of bigger grains (micron size) in agreement with the size inferred from the scattered phase function [97] but at odd with respect to the SED. The flux measurements in scattered

light either from photometry or from spectroscopy are usually difficult to reconcile with thermal emission derived from SED modeling for instance or from ALMA observations. More work towards combining multiwavelength observations is highly desirable.

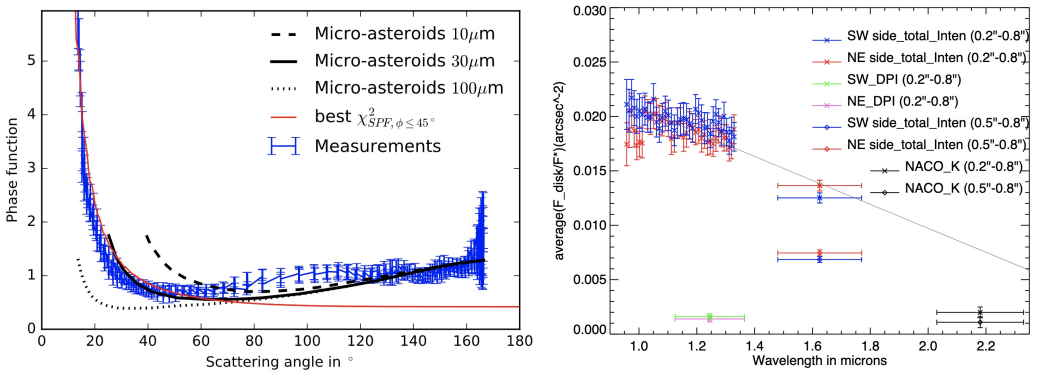

Figure 7. Exemple of a scattering phase function (left) measured in total intensity in the disk of HR 4796 [97], and of a near IR spectrum of HD 32297 [54].

4.4. *Variability and late type stars*

The exquisite resolution of SPHERE allows to obtain consistent measurements at several epochs to perform dynamical studies in debris disks. SPHERE has revealed an unexpected phenomenon in the one of a kind disk around the M-type star AU Mic which is young and ideally located at about 10 pc. Large structures forming some arches a few AU wide were observed during SPHERE commissioning in 2014 on one side of this edge-on debris disk [117]. Not only the structures were all recovered in older data from HST (2010, 2011) but they featured an apparent motion, the interpretation of which is complicated by the edge-on orientation. Follow up observations in the next years confirmed the evidence of the motion, and discovered other smaller structures in different places of the disk, all being moving over time [118] (Fig. 8). Two characteristics were important to understand the behavior of the structures: first they are moving on straight trajectories (linear with time), and the most distant (in apparent projection) are even faster than the escape velocity. All together, some dust particles are blown away from the system, a particularity that was only expected for A-type star owing to the radiation pressure. For AU Mic, being a very active M-type star, the motion of the dust is very likely correlated with its strong stellar winds [119]. In addition, since we observe these structures in specific regions of the disk, it is not a uniform mechanism, so another object is necessarily involved to break the symmetry, possibly being a planet or a local reservoir of dust. Interestingly, the presence of at least two planets was confirmed with transit and radial velocity [120, 121], although they are orbiting too close to the star to be involved in the production of the fast-moving dust features, because of timescale reasons. Whether the same phenomenon can be observed in other M-star systems is still to be determined.

5. Conclusion

Improving the angular resolution of instruments generally comes with higher contrasts. In that respect, SPHERE has been able to achieve significantly larger and more stable contrasts than

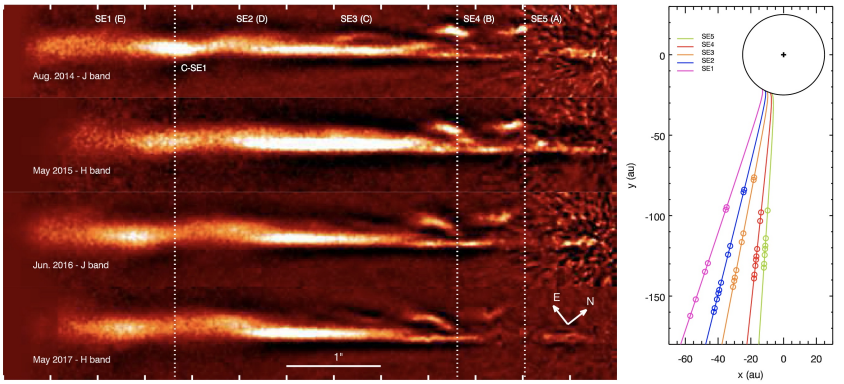

Figure 8. The edge-on disk of AU Mic observed at four epochs (left) showing the fast motion of five extended dust structures (SE1 to SE5). The star is at the right edge of each panel. The right panel displays a possible model with a planet at 34 au [118].

the previous instruments generation. At the same time, some dedicated observing modes were specifically designed for disk science, allowing imaging in total intensity and polarimetry with a rather large field of view both in the visible and near IR, as well as spectro-imaging at low spectral resolution.

These unique capabilities have literally boosted the science on disks at very high angular resolution, and then also provided a mean to characterize in the very details the environment in which planet form. Emblematic structures like spirals, gaps, rings or shadows, were observed in planet forming disks with a precision never achieved before, leading to the identification of clear categories of objects likely reminiscent of different evolutionary states. For the first time, we have been able to witness directly the link between disks and exoplanets but objects like PDS 70 are rare since only a few are observable with SPHERE.

For more mature disks, providing some assumptions on the morphology we are now able to infer optical properties of the dust particles based on spectral reflectance measurements and phase function measurements. Here also both polarimetric and non polarimetric imaging were find crucial to bring the interpretation of debris disks data to a higher level than before. Still, the comparison to models is not fully satisfactory and some works are definitely needed toward reconciling the theory of dust scattering with observations. The extreme stability of SPHERE has enabled the investigation of morphological variability, which at least was possible in two cases: First, when the source of variability is located at short physical distances to be able to detect Keplerian motion in just a few months, as we observed with some shadows in young disks. Second, for the particular case of a very active flaring star, like AU Mic.

As of now, we understand the limitations of SPHERE and other equivalent instruments, so we can foresee the next steps in the form of upgrades or future instruments on the Extremely Large Telescope. An upgrade of SPHERE is proposed to boost exoplanet and disk science, in particular by pushing the contrast further in to detect and to characterize planets and dust structures at close angular separations corresponding to physical separations where we expect planets to form. A second objective is to allow the observations of fainter and redder stars to observe more PDS 70 and AU Mic analogs and also to reinforce the synergy with ALMA observations sensitive to sub millimeter dust grains.

A completely new field in disk science at high angular resolution and high contrast is now

being opened with the James Webb Space Telescope, in particular in the $5-30\,\mu$m spectral range. By providing different types of observables, JWST is intermediate, hence complementary, to scattered light observations in the visible and near IR, and thermal emissions from the dust and gas observed at sub-millimeter. Altogether, these three different regimes will certainly revolutionize our understanding of the birthplace of planets.

Conflicts of interest

The author has no conflict of interest to declare.

References

[1] S. Ida, T. Guillot, A. Morbidelli, "The radial dependence of pebble accretion rates: A source of diversity in planetary systems. I. Analytical formulation", *Astron. Astrophys.* **591** (2016), article no. A72.

[2] E. Kokubo, S. Ida, "Formation of Protoplanets from Planetesimals in the Solar Nebula", *Icarus* **143** (2000), no. 1, p. 15-27.

[3] P. J. Armitage, J. A. Eisner, J. B. Simon, "Prompt Planetesimal Formation beyond the Snow Line", *Astrophys. J.* **828** (2016), no. 1, article no. L2.

[4] E. Kokubo, S. Ida, "Oligarchic Growth of Protoplanets", *Icarus* **131** (1998), no. 1, p. 171-178.

[5] J. B. Pollack, O. Hubickyj, P. Bodenheimer *et al.*, "Formation of the Giant Planets by Concurrent Accretion of Solids and Gas", *Icarus* **124** (1996), no. 1, p. 62-85.

[6] D. Hollenbach, D. Johnstone, S. Lizano, F. Shu, "Photoevaporation of Disks around Massive Stars and Application to Ultracompact H II Regions", *Astrophys. J.* **428** (1994), p. 654-669.

[7] S. N. Raymond, A. Izidoro, A. Morbidelli, "Solar System Formation in the Context of Extrasolar Planets", in *Planetary Astrobiology* (V. S. Meadows, G. N. Arney, B. E. Schmidt, D. J. Des Marais, eds.), University of Arizona Press, 2020, p. 287.

[8] A. P. Boss, "Giant planet formation by gravitational instability", *Science* **276** (1997), p. 1836-1839.

[9] C. Mordasini, Y. Alibert, W. Benz, "Extrasolar planet population synthesis. I. Method, formation tracks, and mass-distance distribution", *Astron. Astrophys.* **501** (2009), no. 3, p. 1139-1160.

[10] K. I. Öberg, R. Murray-Clay, E. A. Bergin, "The Effects of Snowlines on C/O in Planetary Atmospheres", *Astrophysical Journal Letters* **743** (2011), no. 1, article no. L16.

[11] W. Kley, R. P. Nelson, "Planet-Disk Interaction and Orbital Evolution", *Annual Review of Astronomy and Astrophysics* **50** (2012), p. 211-249.

[12] M. C. Wyatt, "Evolution of Debris Disks", *Annual Review of Astronomy and Astrophysics* **46** (2008), no. 1, p. 339-383.

[13] H. H. Aumann, F. C. Gillett, C. A. Beichman *et al.*, "Discovery of a shell around alpha Lyrae", *Astrophysical Journal Letters* **278** (1984), p. L23-L27.

[14] D. E. Backman, F. Paresce, "Main-sequence stars with circumstellar solid material - The VEGA phenomenon", in *Protostars and planets III (A93-42937 17-90)*, University of Arizona Press, 1993, p. 1253-1304.

[15] P. Artymowicz, M. C. Clampin, "Dust around Main-Sequence Stars: Nature or Nurture by the Interstellar Medium?", *Astrophys. J.* **490** (1997), no. 2, p. 863-878.

[16] B. A. Smith, R. J. Terrile, "A Circumstellar Disk around β Pictoris", *Science* **226** (1984), no. 4681, p. 1421-1424.

[17] A. J. Weinberger, E. E. Becklin, G. Schneider *et al.*, "The Circumstellar Disk of HD 141569 Imaged with NICMOS", *Astrophys. J.* **525** (1999), no. 1, p. L53-L56.

[18] J.-C. Augereau, A.-M. Lagrange, D. Mouillet, F. M. Ménard, "HST/NICMOS2 observations of the HD 141569 A circumstellar disk", *Astron. Astrophys.* **350** (1999), p. L51-L54.

[19] J.-C. Augereau, A.-M. Lagrange, D. Mouillet, F. M. Ménard, "HST/NICMOS2 coronagraphic observations of the circumstellar environment of three old PMS stars: HD 100546, SAO 206462 and MWC 480", *Astron. Astrophys.* **365** (2001), no. 2, p. 78-89.

[20] G. Schneider, B. A. Smith, E. E. Becklin *et al.*, "NICMOS Imaging of the HR 4796A Circumstellar Disk", *Astrophys. J.* **513** (1999), no. 2, p. L127-L130.

[21] A. Boccaletti, J.-C. Augereau, F. Marchis, J. Hahn, "Ground-based Near-Infrared Imaging of the HD 141569 Circumstellar Disk", *Astrophys. J.* **585** (2003), no. 1, p. 494-501.

[22] M. C. Clampin, J. E. Krist, D. R. Ardila *et al.*, "Hubble Space Telescope ACS Coronagraphic Imaging of the Circumstellar Disk around HD 141569A", *Astron. J.* **126** (2003), no. 1, p. 385-392.

[23] S. P. Quanz, H. M. Schmid, K. Geissler *et al.*, "Very Large Telescope/NACO Polarimetric Differential Imaging of HD100546—Disk Structure and Dust Grain Properties between 10 and 140 AU", *Astrophys. J.* **738** (2011), no. 1, article no. 23.

[24] S. P. Quanz, H. Avenhaus, E. Buenzli *et al.*, "Gaps in the HD 169142 Protoplanetary Disk Revealed by Polarimetric Imaging: Signs of Ongoing Planet Formation?", *Astrophysical Journal Letters* **766** (2013), no. 1, article no. L2.
[25] A. Boccaletti, J.-C. Augereau, P. Baudoz, E. Pantin, A.-M. Lagrange, "VLT/NACO coronagraphic observations of fine structures in the disk of β Pictoris", *Astron. Astrophys.* **495** (2009), no. 2, p. 523-535.
[26] P. G. Kalas, J. R. Graham, M. C. Clampin, "A planetary system as the origin of structure in Fomalhaut's dust belt", *Nature* **435** (2005), no. 7045, p. 1067-1070.
[27] P. G. Kalas, J. R. Graham, M. C. Clampin, M. P. Fitzgerald, "First Scattered Light Images of Debris Disks around HD 53143 and HD 139664", *Astrophys. J.* **637** (2006), no. 1, p. L57-L60.
[28] P. G. Kalas, M. P. Fitzgerald, J. R. Graham, "Discovery of Extreme Asymmetry in the Debris Disk Surrounding HD 15115", *Astrophys. J.* **661** (2007), no. 1, p. L85-L88.
[29] J. E. Krist, K. R. Stapelfeldt, D. A. Golimowski *et al.*, "Hubble Space Telescope ACS Images of the GG Tauri Circumbinary Disk", *Astron. J.* **130** (2005), no. 6, p. 2778-2787.
[30] G. Schneider, C. A. Grady, D. C. Hines *et al.*, "Probing for Exoplanets Hiding in Dusty Debris Disks: Disk Imaging, Characterization, and Exploration with HST/STIS Multi-roll Coronagraphy", *Astron. J.* **148** (2014), no. 4, article no. 59.
[31] G. Chauvin, A.-M. Lagrange, C. Dumas *et al.*, "A giant planet candidate near a young brown dwarf. Direct VLT/NACO observations using IR wavefront sensing", *Astron. Astrophys.* **425** (2004), p. L29-L32.
[32] A.-M. Lagrange, D. Gratadour, G. Chauvin *et al.*, "A probable giant planet imaged in the β Pictoris disk. VLT/NaCo deep L'-band imaging", *Astron. Astrophys.* **493** (2009), no. 2, p. L21-L25.
[33] A.-M. Lagrange, M. Bonnefoy, G. Chauvin *et al.*, "A Giant Planet Imaged in the Disk of the Young Star β Pictoris", *Science* **329** (2010), no. 5987, p. 57-59.
[34] C. Marois, B. Macintosh, T. Barman *et al.*, "Direct Imaging of Multiple Planets Orbiting the Star HR 8799", *Science* **322** (2008), no. 5906, p. 1348-1352.
[35] C. Marois, B. Zuckerman, Q. M. Konopacky, B. Macintosh, T. Barman, "Images of a fourth planet orbiting HR 8799", *Nature* **468** (2010), no. 7, p. 1080-1083.
[36] P. G. Kalas, J. R. Graham, E. Chiang *et al.*, "Optical Images of an Exosolar Planet 25 Light-Years from Earth", *Science* **322** (2008), no. 5, p. 1345-1348.
[37] G. Chauvin, "Imagerie directe des exoplanètes : résultats et perspectives", *C. R. Phys.* **24** (2023), no. S2, Forthcoming.
[38] F. Cantalloube, C. Gomez-Gonzalez, O. Absil *et al.*, "Exoplanet Imaging Data Challenge: benchmarking the various image processing methods for exoplanet detection", https://arxiv.org/abs/2101.05080, 2021.
[39] J.-L. Beuzit, A. Vigan, D. Mouillet *et al.*, "SPHERE: the exoplanet imager for the Very Large Telescope", *Astron. Astrophys.* **631** (2019), article no. A155.
[40] B. Macintosh, J. R. Graham, P. Ingraham *et al.*, "First light of the Gemini Planet Imager", *Proceedings of the National Academy of Science* **111** (2014), no. 35, p. 12661-12666.
[41] J. Lozi, O. Guyon, N. Jovanovic *et al.*, "SCExAO, an instrument with a dual purpose: perform cutting-edge science and develop new technologies", in *Adaptive Optics Systems VI* (L. M. Close, L. Schreiber, D. Schmidt, eds.), Society of Photo-Optical Instrumentation Engineers (SPIE) Conference Series, vol. 10703, SPIE, 2018.
[42] S. M. Andrews, J. Huang, L. M. Pérez *et al.*, "The Disk Substructures at High Angular Resolution Project (DSHARP). I. Motivation, Sample, Calibration, and Overview", *Astrophysical Journal Letters* **869** (2018), article no. L41.
[43] A. Partnership, C. L. Brogan, L. M. Pérez *et al.*, "THE 2014 ALMA long baseline campaign: first results from high angular resolution observations toward the HL Tau region", *Astrophysical Journal Letters* **808** (2015), no. 1, article no. L3.
[44] J.-F. Sauvage, T. Fusco, C. Petit *et al.*, "SAXO: the extreme adaptive optics system of SPHERE (I) system overview and global laboratory performance", *Journal of Astronomical Telescopes, Instruments, and Systems* **2** (2016), no. 2, article no. 025003.
[45] R. Galicher, J. Mazoyer, "Imager des exoplanètes grâce aux instruments coronographiques", *C. R. Phys.* **24** (2023), no. S2, Forthcoming.
[46] M. Carbillet, P. Bendjoya, L. Abe *et al.*, "Apodized Lyot coronagraph for SPHERE/VLT. I. Detailed numerical study", *Experimental Astronomy* **30** (2011), no. 1, p. 39-58.
[47] É. Choquet, L. Pueyo, J. B. Hagan *et al.*, "Archival legacy investigations of circumstellar environments: overview and first results", in *Space Telescopes and Instrumentation 2014: Optical, Infrared, and Millimeter Wave* (J. M. J. Oschmann, M. C. Clampin, G. G. Fazio, H. A. MacEwen, eds.), Society of Photo-Optical Instrumentation Engineers (SPIE) Conference Series, vol. 9143, SPIE, 2014.
[48] É. Choquet, M. D. Perrin, C. H. H. Chen *et al.*, "First Images of Debris Disks around TWA 7, TWA 25, HD 35650, and HD 377", *Astrophysical Journal Letters* **817** (2016), no. 1, article no. L2.
[49] C. Xie, É. Choquet, A. Vigan *et al.*, "Reference-star differential imaging on SPHERE/IRDIS", https://arxiv.org/abs/2208.07915, 2022.
[50] C. Marois, D. Lafrenière, R. Doyon, B. Macintosh, D. Nadeau, "Angular Differential Imaging: A Powerful High-Contrast Imaging Technique", *Astrophys. J.* **641** (2006), no. 1, p. 556-564.

[51] D. Lafreniere, C. Marois, R. Doyon, D. Nadeau, É. Artigau, "A New Algorithm for Point-Spread Function Subtraction in High-Contrast Imaging: A Demonstration with Angular Differential Imaging", *Astrophys. J.* **660** (2007), no. 1, p. 770-780.
[52] R. Soummer, L. Pueyo, J. E. Larkin, "Detection and Characterization of Exoplanets and Disks Using Projections on Karhunen-Loève Eigenimages", *Astrophysical Journal Letters* **755** (2012), no. 2, article no. L28.
[53] J. Milli, D. Mouillet, A.-M. Lagrange *et al.*, "Impact of angular differential imaging on circumstellar disk images", *Astron. Astrophys.* **545** (2012), article no. A111.
[54] T. Bhowmik, A. Boccaletti, P. Thébault *et al.*, "Spatially resolved spectroscopy of the debris disk HD 32297", *Astron. Astrophys.* **630** (2019), article no. A85.
[55] O. Flasseur, S. Thé, L. Denis, É. Thiébaut, M. Langlois, "REXPACO: An algorithm for high contrast reconstruction of the circumstellar environment by angular differential imaging", *Astron. Astrophys.* **651** (2021), article no. A62.
[56] B. Pairet, F. Cantalloube, L. Jacques, "MAYONNAISE: a morphological components analysis pipeline for circumstellar discs and exoplanets imaging in the near-infrared", *Mon. Not. Roy. Astron. Soc.* **503** (2021), no. 3, p. 3724-3742.
[57] C. Thalmann, M. Janson, E. Buenzli *et al.*, "Images of the Extended Outer Regions of the Debris Ring around HR 4796 A", *Astrophysical Journal Letters* **743** (2011), no. 1, article no. L6.
[58] A. Garufi, S. P. Quanz, H. M. Schmid *et al.*, "The SPHERE view of the planet-forming disk around HD 100546", *Astron. Astrophys.* **588** (2016), article no. A8.
[59] R. van Boekel, R. G. van Holstein, J. H. V. Girard *et al.*, "Polarimetric imaging mode of VLT/SPHERE/IRDIS", *Astron. Astrophys.* **633** (2020), article no. A64.
[60] J. de Boer, M. Langlois, R. van Boekel, R. G. van Holstein *et al.*, "Polarimetric imaging mode of VLT/SPHERE/IRDIS", *Astron. Astrophys.* **633** (2020), article no. A63.
[61] A. Garufi, M. Benisty, T. Stolker *et al.*, "Three years of SPHERE: the latest view of the morphology and evolution of protoplanetary discs", *The Messenger* **169** (2017), p. 32-37.
[62] D. A. Golimowski, D. R. Ardila, J. E. Krist *et al.*, "Hubble Space Telescope ACS Multiband Coronagraphic Imaging of the Debris Disk around β Pictoris", *Astron. J.* **131** (2006), no. 6, p. 3109-3130.
[63] R. Dong, Z. Zhu, R. R. Rafikov, J. M. Stone, "Observational Signatures of Planets in Protoplanetary Disks: Spiral Arms Observed in Scattered Light Imaging Can Be Induced by Planets", *Astrophysical Journal Letters* **809** (2015), no. 1, article no. L5.
[64] M. Benisty, A. Juhasz, A. Boccaletti *et al.*, "Asymmetric features in the protoplanetary disk MWC 758", *Astron. Astrophys.* **578** (2015), article no. L6.
[65] R. R. Rafikov, "Nonlinear Propagation of Planet-generated Tidal Waves", *Astrophys. J.* **569** (2002), no. 2, p. 997-1008.
[66] T. Muto, C. A. Grady, J. Hashimoto *et al.*, "Discovery of Small-scale Spiral Structures in the Disk of SAO 206462 (HD 135344B): Implications for the Physical State of the Disk from Spiral Density Wave Theory", *Astrophysical Journal Letters* **748** (2012), no. 2, article no. L22.
[67] T. Stolker, C. Dominik, H. Avenhaus *et al.*, "Shadows cast on the transition disk of HD 135344B", *Astron. Astrophys.* **595** (2016), article no. A113.
[68] A.-L. Maire, T. Stolker, S. Messina *et al.*, "Testing giant planet formation in the transitional disk of SAO 206462 using deep VLT/SPHERE imaging", *Astron. Astrophys.* **601** (2017), article no. A134.
[69] A. Boccaletti, E. Pantin, F. M. Ménard *et al.*, "Investigating point sources in MWC 758 with SPHERE", *Astron. Astrophys.* **652** (2021), article no. L8.
[70] K. Wagner, D. Apai, M. Kasper, M. Robberto, "Discovery of a Two-armed Spiral Structure in the Gapped Disk around Herbig Ae Star HD 100453", *Astrophysical Journal Letters* **813** (2015), no. 1, article no. L2.
[71] R. Dong, Z. Zhu, J. Fung *et al.*, "An M Dwarf Companion and Its Induced Spiral Arms in the HD 100453 Protoplanetary Disk", *Astrophysical Journal Letters* **816** (2016), no. 1, article no. L12.
[72] Y.-W. Tang, S. Guilloteau, A. Dutrey *et al.*, "Planet Formation in AB Aurigae: Imaging of the Inner Gaseous Spirals Observed inside the Dust Cavity", *Astrophys. J.* **840** (2017), no. 1, article no. 32.
[73] A. Boccaletti, E. di Folco, E. Pantin *et al.*, "Possible evidence of ongoing planet formation in AB Aurigae. A showcase of the SPHERE/ALMA synergy", *Astron. Astrophys.* **637** (2020), article no. L5.
[74] T. Currie, K. Lawson, G. Schneider *et al.*, "Images of embedded Jovian planet formation at a wide separation around AB Aurigae", *Nature Astronomy* (2022), p. 1-9.
[75] R. Gratton, R. Ligi, E. Sissa *et al.*, "Blobs, spiral arms, and a possible planet around HD 169142", *Astron. Astrophys.* **623** (2019), article no. A140.
[76] B. Ren, R. Dong, R. G. van Holstein *et al.*, "Dynamical Evidence of a Spiral Arm–driving Planet in the MWC 758 Protoplanetary Disk", *Astrophys. J.* **898** (2020), no. 2, article no. L38.
[77] M. Langlois, A. Pohl, A.-M. Lagrange *et al.*, "First scattered light detection of a nearly edge-on transition disk around the T Tauri star RY Lupi", *Astron. Astrophys.* **614** (2018), article no. A88.
[78] A. Pohl, E. Sissa, M. Langlois *et al.*, "New constraints on the disk characteristics and companion candidates around T Chamaeleontis with VLT/SPHERE", *Astron. Astrophys.* **605** (2017), article no. A34.

[79] R. Dong, C. Hall, K. Rice, E. Chiang, "Spiral Arms in Gravitationally Unstable Protoplanetary Disks as Imaged in Scattered Light", *Astrophysical Journal Letters* **812** (2015), no. 2, article no. L32.
[80] R. van Boekel, T. Henning, J. Menu *et al.*, "Three Radial Gaps in the Disk of TW Hydrae Imaged with SPHERE", *Astrophys. J.* **837** (2017), no. 2, article no. 132.
[81] T. Meshkat, V. P. Bailey, K. Y. L. Su *et al.*, "Searching for Planets in Holey Debris Disks with the Apodizing Phase Plate", *Astrophys. J.* **800** (2015), no. 1, article no. 5.
[82] C. Ginski, T. Stolker, P. Pinilla *et al.*, "Direct detection of scattered light gaps in the transitional disk around HD 97048 with VLT/SPHERE", *Astron. Astrophys.* **595** (2016), article no. A112.
[83] J. de Boer, G. Salter, M. Benisty *et al.*, "Multiple rings in the transition disk and companion candidates around RX J1615.3-3255", *Astron. Astrophys.* **595** (2016), p. A114.
[84] R. Ligi, A. Vigan, R. Gratton *et al.*, "Investigation of the inner structures around HD 169142 with VLT/SPHERE", *Mon. Not. Roy. Astron. Soc.* **473** (2017), no. 2, p. 1774-1783.
[85] Y. Zhang, L. Jin, "The evolution of the snow line in a protoplanetary disk", *Astrophys. J.* **802** (2015), no. 1, article no. 58.
[86] R. U. Claudi, A.-L. Maire, D. Mesa *et al.*, "SPHERE dynamical and spectroscopic characterization of HD 142527B", *Astron. Astrophys.* **622** (2018), article no. A96.
[87] M. Keppler, A. Penzlin, M. Benisty *et al.*, "Gap, shadows, spirals, and streamers: SPHERE observations of binary-disk interactions in GG Tauri A", *Astron. Astrophys.* **639** (2020), article no. A62.
[88] M. Keppler, M. Benisty, A. Müller *et al.*, "Discovery of a planetary-mass companion within the gap of the transition disk around PDS 70", *Astron. Astrophys.* **617** (2018), article no. A44.
[89] A. Müller, M. Keppler, T. Henning *et al.*, "Orbital and atmospheric characterization of the planet within the gap of the PDS 70 transition disk", *Astron. Astrophys.* **617** (2018), article no. L2.
[90] S. Y. Haffert, A. J. Bohn, J. de Boer *et al.*, "Two accreting protoplanets around the young star PDS 70", *Nature Astronomy* **3** (2019), p. 749-754.
[91] D. Mesa, M. Keppler, F. Cantalloube *et al.*, "VLT/SPHERE exploration of the young multiplanetary system PDS70", *Astron. Astrophys.* **632** (2019), article no. A25.
[92] M. Benisty, J. Bae, S. Facchini *et al.*, "A Circumplanetary Disk around PDS70c", *Astrophysical Journal Letters* **916** (2021), no. 1, article no. L2.
[93] S. Hunziker, H. M. Schmid, J. Ma *et al.*, "HD 142527: quantitative disk polarimetry with SPHERE", *Astron. Astrophys.* **648** (2021), article no. A110.
[94] H. Avenhaus, S. P. Quanz, H. M. Schmid *et al.*, "Structures in the Protoplanetary Disk of HD142527 Seen in Polarized Scattered Light", *Astrophys. J.* **781** (2014), no. 2, article no. 87.
[95] S. Marino, S. Perez, S. Casassus, "Shadows Cast by a Warp in the HD 142527 Protoplanetary Disk", *Astrophysical Journal Letters* **798** (2015), no. 2, article no. L44.
[96] M. Benisty, T. Stolker, A. Pohl *et al.*, "Shadows and spirals in the protoplanetary disk HD 100453", *Astron. Astrophys.* **597** (2017), article no. A42.
[97] J. Milli, A. Vigan, D. Mouillet *et al.*, "Near-infrared scattered light properties of the HR 4796 A dust ring", *Astron. Astrophys.* **599** (2017), article no. A108.
[98] J. Wisdom, "The resonance overlap criterion and the onset of stochastic behavior in the restricted three-body problem", *Astron. J.* **85** (1980), p. 1122-1133.
[99] E. J. Lee, E. Chiang, "A Primer on Unifying Debris Disk Morphologies", *Astrophys. J.* **827** (2016), no. 2, article no. 125.
[100] D. Mouillet, J. D. Larwood, J. C. B. Papaloizou, A.-M. Lagrange, "A planet on an inclined orbit as an explanation of the warp in the β Pictoris disc", *Mon. Not. Roy. Astron. Soc.* **292** (1997), p. 896-904.
[101] P. G. Kalas, A. Rajan, J. J. Wang *et al.*, "Direct Imaging of an Asymmetric Debris Disk in the HD 106906 Planetary System", *Astrophys. J.* **814** (2015), no. 1, article no. 32.
[102] A.-M. Lagrange, M. Langlois, R. Gratton *et al.*, "A narrow, edge-on disk resolved around HD 106906 with SPHERE", *Astron. Astrophys.* **586** (2016), article no. L8.
[103] M. Feldt, J. Olofsson, A. Boccaletti *et al.*, "SPHERE/SHINE reveals concentric rings in the debris disk of HIP 73145", *Astron. Astrophys.* **601** (2017), article no. A7.
[104] A. Boccaletti, P. Thébault, N. Pawellek *et al.*, "Two cold belts in the debris disk around the G-type star NZ Lupi", *Astron. Astrophys.* **625** (2019), article no. A21.
[105] M. Bonnefoy, J. Milli, F. M. Ménard *et al.*, "Belt(s) of debris resolved around the Sco-Cen star HIP 67497", *Astron. Astrophys.* **597** (2017), article no. L7.
[106] C. Perrot, A. Boccaletti, E. Pantin *et al.*, "Discovery of concentric broken rings at sub-arcsec separations in the HD 141569A gas-rich, debris disk with VLT/SPHERE", *Astron. Astrophys.* **590** (2016), article no. L7.
[107] W. Lyra, M. J. Kuchner, "Formation of sharp eccentric rings in debris disks with gas but without planets", *Nature* **499** (2013), no. 7457, p. 184-187.
[108] E. Di Folco, J. Péricaud, A. Dutrey *et al.*, "An ALMA/NOEMA study of gas dissipation and dust evolution in the 5 Myr-old HD 141569A hybrid disc⋆", *Astron. Astrophys.* **635** (2020), article no. A94.

[109] G. Singh, T. Bhowmik, A. Boccaletti *et al.*, "Revealing asymmetrical dust distribution in the inner regions of HD 141569", *Astron. Astrophys.* **653** (2021), article no. A79.

[110] Q. Kral, S. Marino, M. C. Wyatt, M. Kama, L. Matrà, "Imaging [CI] around HD 131835: reinterpreting young debris discs with protoplanetary disc levels of CO gas as shielded secondary discs", *Mon. Not. Roy. Astron. Soc.* **489** (2019), no. 34, p. 3670-3691.

[111] A. P. Jackson, M. C. Wyatt, A. Bonsor, D. Veras, "Debris froms giant impacts between planetary embryos at large orbital radii", *Mon. Not. Roy. Astron. Soc.* **440** (2014), no. 4, p. 3757-3777.

[112] J. Olofsson, J. Milli, A. Bayo, T. Henning, N. Engler, "The challenge of measuring the phase function of debris discs", *Astron. Astrophys.* **640** (2020), article no. A12.

[113] J. Milli, N. Engler, H. M. Schmid *et al.*, "Optical polarised phase function of the HR 4796A dust ring", *Astron. Astrophys.* **626** (2019), article no. A54.

[114] C. Adam, J. Olofsson, S. Guilloteau *et al.*, "Characterizing the morphology of the debris disk around the low-mass star GSC 07396-00759", *Astron. Astrophys.* **653** (2021), article no. A88.

[115] N. Engler, A. Boccaletti, H. M. Schmid *et al.*, "Investigating the presence of two belts in the HD 15115 system", *Astron. Astrophys.* **622** (2019), article no. A192.

[116] A. C. Levasseur-Regourd, C. Baruteau, J. Lasue, J. Milli, J.-B. Renard, "Linking studies of tiny meteoroids, zodiacal dust, cometary dust and circumstellar disks", *Planetary and Space Science* **186** (2020), article no. 104896.

[117] A. Boccaletti, C. Thalmann, A.-M. Lagrange *et al.*, "Fast-moving features in the debris disk around AU Microscopii", *Nature* **526** (2015), no. 7572, p. 230-232.

[118] A. Boccaletti, E. Sezestre, A.-M. Lagrange *et al.*, "Observations of fast-moving features in the debris disk of AU Mic on a three-year timescale: Confirmation and new discoveries", *Astron. Astrophys.* **614** (2018), article no. A52.

[119] E. Sezestre, J.-C. Augereau, A. Boccaletti, P. Thébault, "Expelled grains from an unseen parent body around AU Microscopii", *Astron. Astrophys.* **607** (2017), article no. A65.

[120] P. Plavchan, T. Barclay, J. Gagné *et al.*, "A planet within the debris disk around the pre-main-sequence star AU Microscopii", *Nature* **582** (2020), no. 7813, p. 497-500.

[121] E. Martioli, G. Hébrard, C. Moutou *et al.*, "Spin-orbit alignment and magnetic activity in the young planetary system AU Mic", *Astron. Astrophys.* **641** (2020), article no. L1.